

What is the order of 2D polymer escape transition?

Hsiao-Ping Hsu and Kurt Binder
*Institut für Physik, Johannes Gutenberg-Universität Mainz
D-55099 Mainz, Staudinger Weg 7, Germany*

Leonid I. Klushin
American University of Beirut, Department of Physics, Beirut, Lebanon

Alexander M. Skvortsov
Chemical-Pharmaceutical Academy, Prof. Popova 14, 197022 St. Petersburg, Russia.
(Dated: February 8, 2022)

An end-grafted flexible polymer chain in 3d space between two pistons undergoes an abrupt transition from a confined coil to a flower-like conformation when the number of monomers in the chain, N , reaches a critical value. In $2d$ geometry, excluded volume interactions between monomers of a chain confined inside a strip of finite length $2L$ transform the coil conformation into a linear string of blobs. However, the blob picture raises questions on the nature of this escape transition. To check the theoretical predictions based on the blob picture we study $2d$ single polymer chains with excluded volume interactions and with one end grafted in the middle of a strip of length $2L$ and width H by simulating self-avoiding walks on a square lattice with the pruned-enriched-Rosenbluth method (PERM). We estimate the free energy, the end-to-end distance, the number of imprisoned monomers, the order parameter, and its distribution. It is shown that in the thermodynamic limit of large N and L but finite L/N , there is a small but finite jump in several average characteristics, including the order parameter. We also present a theoretical description based on the Landau free energy approach, which is in good agreement with the simulation results. Both simulation results and the analytical theory indicate that the $2d$ escape transition is a weak first-order phase transition.

I. INTRODUCTION

A phenomenon that was called escape transition occurs upon progressive squeezing an end-grafted polymer chain between two pistons and has attracted great interest [1-16]. At weak deformation the chain is compressed uniformly into a relatively thick pan-cake conformation. Beyond certain critical compression, the chain configuration changes abruptly. One part of the chain forms a stem stretching from the grafting point to the piston edge, while the rest of the segments form a coiled crown outside the piston, thus escaping from the region underneath the piston. An abrupt change from one state to another implies a first order transition. Various aspects of this problem were investigated: The escape transition of compressed polymer mushrooms in 3d space was investigated thoroughly by scaling theory [1], numerical calculations [2, 3, 4], and computer modeling under good solvent [5], and theta solvent [6] conditions. The escape transition of star polymers was discussed in [7], and the escape transition of di-block-copolymers was considered in [8]. The influence of the curvature of the pistons was investigated in [9, 10], and the effect of adsorption between the polymer chain and the surface of the piston was considered in [11]. A comparison between Monte Carlo simulations and experimental results by atomic force-electrochemical microscopy was recently presented in [12]. A rigorous analytical theory for the equilibrium and kinetic aspects of the escape transition for a Gaussian chain was constructed in [13, 14]. Metastability effects, negative compressibility and the nonequivalence of

the escape transition in two conjugate ensembles were analyzed for the same model in [15, 16].

The reason for studying the escape transition is that it gives the possibility to understand the phenomenon of a very unconventional phase transition. The concept of a phase transition requires taking a thermodynamic limit. For standard low-molecular weight systems as well as for macromolecular systems in condensed bulk matter finite size effects are usually negligible. In contrast to that, phase transitions at the level of a single macromolecule e.g., the coil-globule transition [17], or polymer adsorption at an interface [18, 19] - do not have any analogies in the physics of low molecular mass systems. A single macromolecule always consists of a finite number of monomers N : computer modeling rarely deals with N larger than 10^4 so that finite-size effects in the single-molecule phase transitions are the rule rather than the exception. The situation is much more complicated in the case of the escape transition. It was shown [1] that the escape transition point (critical compression) depends on the relation between the chain length Na (a is the distance between neighboring monomers) and the piston radius L . Therefore, to analyze the escape transition in the thermodynamic limit, it is necessary to take both $Na \rightarrow \infty$ and $L \rightarrow \infty$ but $Na/L = \text{const}$.

The physics of phase transitions is generally known to be strongly affected by the spatial dimensionality. For phase transitions at the level of a single macromolecule the spatial dimensionality is important because excluded volume effects are especially large for polymeric chains in two dimensions [20]. An ideal chain without excluded

volume interactions retains a Gaussian coil conformation with the lateral size $\sim N^{1/2}$ even when it is confined in a 2d strip. There is a very pronounced difference between this state and the partially escaped state with a strongly stretched stem of size $L \sim Na$. On the contrary, a 2d polymer chain with excluded volume interactions confined in a strip is already strongly elongated with the size $\sim Na$. It is not clear whether the difference between the confined and the escaped states is large enough to result in a phase transition.

To analyze the excluded volume effects of the escape transition, we study a flexible polymer chain containing N links of length a (N monomers) grafted in the middle of a strip of length $2L$ and width H , under good solvent conditions. Schematic drawings of a polymer chain in an imprisoned state and in an escaped state are shown in Fig. 1. First, we summarize the results of the escape transition for a 2d Gaussian ideal chain in Sec. II, and then we give the theoretical predictions based on the blob picture in Sec. III. In an experimental setup, the escape transition is driven by changing the piston separation H , while in a blob picture, the escape transition is studied by changing the chain length N or the strip length L at fixed H which is also the size of a blob. Comparisons between the escape transition behavior of the Gaussian chain model and that of the blob model in the thermodynamic limit are given in Sec. IV. In Sec. V we present our results from Monte Carlo (MC) simulations with the pruned-enriched Rosenbluth method (PERM) [21]. In Sec. VI we provide a theoretical description based on the Landau free energy approach which is compared with MC results. A summary and discussions are given in Sec. VII. Detailed analyses of the variances of the imprisoned monomers are given in the Appendix.

II. ESCAPE FOR A 2D GAUSSIAN CHAIN

For the escape transition of a Gaussian chain, a closed-form of the exact partition function was obtained earlier in [14]. The asymptotic form of the free energy F has two branches:

$$F = \begin{cases} N \frac{1}{2d} \left(\frac{\pi a}{H} \right)^2 = F_{\text{imp}} & \text{imprisoned state} \\ \frac{\pi L}{H} = F_{\text{esc}} & \text{escaped state} \end{cases} \quad (1)$$

Here d is the dimensionality of space and a factor of $k_B T$ is absorbed in the free energy throughout the paper. It was shown by direct numerical comparison that the simple asymptotic expressions provide a very accurate description. The two branches meet at the transition point which is given by

$$\left(\frac{L}{Na} \right)^{**} = \frac{\pi}{2d} \frac{a}{H}, \quad \text{with } d = 2. \quad (2)$$

The average lateral forces acting on the grafting point are obtained by

$$f_L = \frac{\partial F(N, L, H)}{\partial L} \quad (3)$$

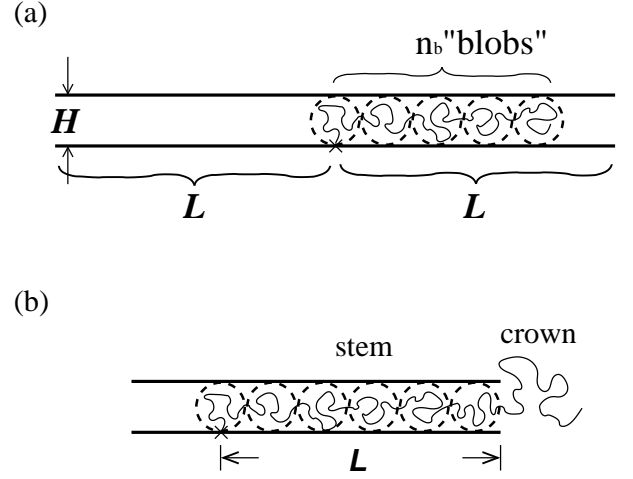


FIG. 1: Schematic drawings of a flexible polymer chain of length N grafted in the middle of the strip of length $2L$ and width H , in a blob picture: (a) As the chain is imprisoned inside the strip, it forms a sequence of n_b blobs. (b) As the chain length is larger than the maximum chain length N^* of a chain in an imprisoned state, the chain partially escapes from the strip and forms an escaped state. A escaped state consists of a “stem” containing N^* monomers and a “crown” containing $N - N^*$ monomers.

which is related to the work required to pull a chain end into confined space by a unit distance. The average compression force

$$f_H = - \frac{\partial F(N, L, H)}{\partial H} \quad (4)$$

is related to the work of compression. It was shown earlier [14] that the average fraction of imprisoned monomers is given by the derivative $N_{\text{imp}} = \partial F(N, L, H) / \partial u$ of the free energy with respect to the effective confining potential $u = (\pi a / 2H)^2$.

The average end-to-end distance per monomer is:

$$\frac{R}{Na} = \begin{cases} N^{-1/2} & \text{imprisoned state} \\ \frac{L}{Na} + N^{-1/2} (1 - N_{\text{imp}}/N)^{1/2} & \text{escaped state} \end{cases} \quad (5)$$

The Landau order parameter s for the escape transition was introduced in [14] as a stretching degree of the chain r_N/N for the imprisoned state and as the stretching degree of the stem L/n_{imp} for the escaped state. Note that the order parameter is defined for an instantaneous configuration with a given end-to-end distance r_N and the number of imprisoned monomers n_{imp} which may be quite different from the equilibrium average values $R = \langle r_N \rangle$ and $N_{\text{imp}} = \langle n_{\text{imp}} \rangle$. The Landau free energy is defined as a function of the order parameter. The Landau free energy for the imprisoned state is just the free energy of a coil as a function of its free end position, which has a standard parabolic form:

$$\Phi_{\text{imp}}(s) = N \left[\frac{d}{2} s^2 + \frac{1}{2d} \left(\frac{\pi a}{H} \right)^2 \right]. \quad (6)$$

At $s = s_{\text{eq}}^{\text{imp}} = 0$, the system is in equilibrium and the corresponding equilibrium free energy, i.e., the depth of the minimum, is $\Phi_{\text{imp}}(0) = (N/2d)(\pi a/H)^2$. For the escaped state,

$$\Phi_{\text{esc}}(s) = \frac{L}{a} \left[\frac{d}{2}s + \frac{1}{2d} \left(\frac{\pi a}{H} \right)^2 \frac{1}{s} \right]. \quad (7)$$

The position of the minimum is at $s = s_{\text{eq}}^{\text{esc}} = \pi a/dH$, and the corresponding depth is $\Phi_{\text{esc}}(s_{\text{eq}}^{\text{esc}}) = \pi L/H$. The binodal is determined by the condition that the two minima are equally deep, i.e. $\Phi_{\text{imp}}(s_{\text{eq}}^{\text{imp}}) = \Phi_{\text{esc}}(s_{\text{eq}}^{\text{esc}})$, which leads to the transition point described by Eq. (2). At the transition point, the average order parameter $S = \langle s \rangle$ jumps from $s_{\text{eq}}^{\text{imp}}$ to $s_{\text{eq}}^{\text{esc}}$. The Landau function allows one to analyze metastable states and to define the two lines where either one of the metastable minima vanishes [16]. Theoretical predictions for the escape transition of a Gaussian chain are summarized in Table I and shown in Fig 2. Detailed discussion and comparison with the prediction from the blob picture for 2d polymer chains are given in Sec. IV.

III. BLOB PICTURE OF A 2D ESCAPE

A free chain in $d = 2$, has an average end-to-end distance given by $\langle a \rangle$ (the distance between neighboring monomers) [17-20]

$$R_F = aN^{3/4} \quad (8)$$

here the prefactors of order unity are neglected throughout. Based on the blob picture we have a cigar of blobs (n_b blobs in total) in the confined situation. Thus the average end-to-end distance is

$$R = n_b(2r_b) = n_b H \quad (9)$$

where r_b is the blob radius. Within a blob, self-avoiding walks (SAW) statistics holds, so if g monomers belong to a blob

$$H = ag^{3/4} = 2r_b, \quad g = (H/a)^{4/3}. \quad (10)$$

Since every monomer of a chain in an imprisoned state must be in a blob we furthermore have

$$N = gn_b = n_b(H/a)^{4/3}, \quad n_b = N(H/a)^{-4/3}. \quad (11)$$

This yields, together with Eq. (9), the formula for the end-to-end distance

$$R/a = N(H/a)^{-1/3} \quad (12)$$

If H is of the same order as R_F , Eq. (8), one finds $R/a = N^{3/4}$, giving a smooth crossover to mushroom behavior, as expected.

The free energy excess of the chain in an imprisoned state (in units of $k_B T$), relative to an unconfined mushroom, is simply the number of blobs, n_b ,

$$F_{\text{imp}} = n_b = N(H/a)^{-4/3} \quad (13)$$

We now define $N = N^*$ as the maximum chain length of an imprisoned chain. Then for $N > N^*$ the chain consists of a “stem” containing N^* imprisoned monomers and an escaped “crown” comprising the rest $N - N^*$ monomers (Fig. 1b). Thus, we find N^* from the condition that R becomes equal to L at the transition point, using Eq. (12)

$$N^* = (L/a)(H/a)^{1/3}. \quad (14)$$

Since the free energy of an unconfined mushroom is taken as zero reference point, the “crown” does not contribute to the excess free energy of the escaped chain, which is hence due to the stem only:

$$F_{\text{esc}} = N^*(H/a)^{-4/3} = L/H. \quad (15)$$

The average end-to-end distance of the escaped chain (in axial direction parallel to the confining boundaries) hence becomes

$$R_{\text{esc}} = L + a(N - N^*)^{3/4}. \quad (16)$$

Equations (13) and (15) show that the free energy as a function of N for fixed H and L , consists of two branches, i.e., F_{imp} for the imprisoned state ($N < N^*$) and F_{esc} for the escaped state ($N > N^*$), meeting at $N = N^*$. The lateral and the compression forces are obtained from the free energy by using Eqs. (3) and (4). We use the same definition of the order parameter s as that for the Gaussian chain, so the average order parameter S

$$S = \langle s \rangle = \begin{cases} R/Na & \text{imprisoned state} \\ L/N^*a = (H/a)^{-1/3} & \text{escaped state} \end{cases}. \quad (17)$$

From Eqs. (12), (14), and (17), we find that the order parameter does not show any discontinuity at the transition, but simply stays constant, i.e. $S = (H/a)^{-1/3}$. Results of the theoretical predictions are listed in Table I and also shown in Fig. 2.

IV. COMPARISON OF THE GAUSSIAN AND BLOB PICTURES

In the thermodynamic limit $N \rightarrow \infty$, $L \rightarrow \infty$, L/N remains as a nontrivial variable along with H . In Fig. 2, theoretical predictions of the Gaussian chain model and of the blob model are shown by dotted and solid lines, respectively. The strip width, H , is fixed, and the ratio L/N is varied. The chain is in an imprisoned state if $\frac{L}{N}$ is larger than the corresponding critical value, $(\frac{L}{N})^{**}$ for the Gaussian chain model or $(\frac{L}{N})^*$ for the blob model, and in the escaped state for $\frac{L}{N} < (\frac{L}{N})^{**}$ [$(\frac{L}{N})^*$]. All curves show only the scaling behavior disregarding numerical coefficients of order one, and the bond length a is taken as a unit length.

In both models, the free energy per monomer is given by piecewise linear functions of L/N . For the escaped

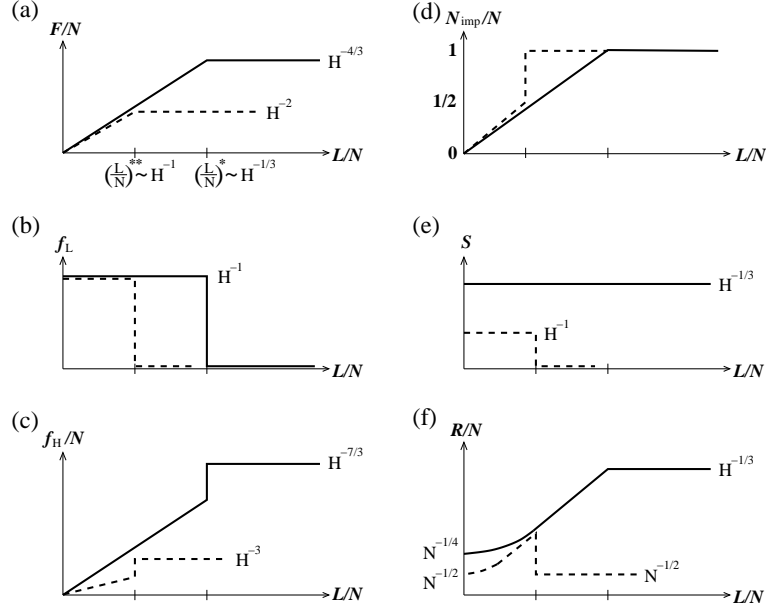


FIG. 2: Theoretical predictions for various averaged chain characteristics plotted against L/N at constant strip width H : (a) the free energy per monomer F/N , (b) the lateral force f_L , (c) the compression force per monomer f_H/N , (d) the fraction of imprisoned monomers N_{imp}/N , (e) the order parameter S , (f) the end-to-end distance per monomer R/N . Gaussian model results are shown by dotted lines, blob model results - by solid lines. The chain is in an imprisoned state for $\frac{L}{N} > (\frac{L}{N})^{**}$ $[(\frac{L}{N})^*]$, and in an escaped state for $\frac{L}{N} < (\frac{L}{N})^{**}$ $[(\frac{L}{N})^*]$ for the Gaussian chain model [blob picture].

TABLE I: Theoretical predictions for the average values of the free energy per monomer F/N , the lateral force f_L , the compression force per monomer f_H/N , the fraction of imprisoned monomers N_{imp}/N , the order parameter S , and the reduced end-to-end distance R/Na based on the Gaussian chain model and the blob picture.

Characteristics of the chain	Imprisoned state		Escaped state	
	Gaussian	Blob	Gaussian	Blob
$\frac{F}{N}$	$(\frac{\pi a}{2H})^2$	$(\frac{a}{H})^{4/3}$	$\frac{\pi}{H} \frac{L}{N}$	$\frac{1}{H} \frac{L}{N}$
f_L	0	0	$\frac{\pi}{H}$	$\frac{1}{H}$
$\frac{f_H}{N}$	$\frac{\pi^2}{2a} (\frac{a}{H})^3$	$\frac{4}{3a} (\frac{a}{H})^{7/3}$	$\frac{\pi}{H^2} \frac{L}{N}$	$\frac{1}{H^2} \frac{L}{N}$
$\frac{N_{\text{imp}}}{N}$	1	1	$\frac{2}{\pi} \frac{H}{a} \frac{L}{Na}$	$(\frac{H}{a})^{1/3} \frac{L}{Na}$
S	0	$(\frac{a}{H})^{1/3}$	$\frac{\pi}{2} \frac{a}{H}$	$(\frac{a}{H})^{1/3}$
$\frac{R}{Na}$	$N^{-1/2}$	$(\frac{H}{a})^{-1/3}$	$N^{-1/2} \left(1 - \frac{N_{\text{imp}}}{N}\right)^{1/2} + \frac{L}{Na}$	$N^{-1/4} \left(1 - \frac{N_{\text{imp}}}{N}\right)^{3/4} + \frac{L}{Na}$

state, the slope of F/N vs. L/N is the same up to numerical coefficients of order 1, and scales as H^{-1} . This slope has the meaning of the lateral force acting on the grafting point. It is proportional to the inverse size of a blob which is defined purely by confinement width H irrespective of whether excluded volume interactions are present or not. The free energy per monomer in the imprisoned state is independent of L/N , and scales as the inverse number of monomers in one blob, $g^{-1} = (a/H)^{1/\nu}$, where ν is the Flory exponent. The transition points in the two models may be quite far apart since they scale differently with H . In the setup where L/N is fixed and the piston separation

is decreasing, the blob model predicts the transition to happen at lower compression, as compared to the Gaussian chain. In both models the lateral force jumps from H^{-1} to zero at the respective transition point. As for compression forces, they are strongly affected by excluded volume interactions (Fig. 2c). The difference in the plateau values for the imprisoned state reflects the lower compressibility of the self-avoiding walk as compared to the Gaussian chain. This corresponds directly to the plateau values of the free energy in Fig. 2a. In the Gaussian chain model, the compression force jumps at the transition point by a factor of 2, while the jump

in the blob model is by a factor of $4/3$.

Figures 2a - 2c suggest that the behavior of both models is fundamentally the same and characteristic of a first-order phase transition. However, the next 3 graphs demonstrate qualitatively different predictions of the Gaussian and the blob models.

For the Gaussian chain model, a transition from the confined state to the escaped state is accompanied by a jump in the average number of imprisoned monomers. At the transition point, one half of the total number of monomers are ejected outside to form a crown, see Fig. 2d. In contrast to that, the blob model predicts a smooth change without a jump. This directly affects the behavior of the average order parameter: while in the Gaussian chain model there is a pronounced jump, the blob model suggests that the order parameter does not change at all. The large constant value of S in the blob model is due to the cigar-shape conformation of the chain in an imprisoned state which is identical to the shape of the stem in the escaped state.

The behavior of the average end-to-end distance is also qualitatively different for the two models. The plateau value for the imprisoned Gaussian chain, $R/N = N^{-1/2}$, is characteristic of the ideal coil, while for the elongated cigar, this ratio is N -independent. The linear part of the curves corresponding to the escaped state simply represents the dominant contribution of the stem to the overall end-to-end distance, $R \approx L$ irrespective of the model. At very low values of L/N corrections due to the crown size become large, as shown in Fig 2f. The size of the Gaussian chain demonstrates a jump at the transition point consistent with a strong conformation change accompanying the first-order transition. In the blob model, the chain size does not have any jump.

It is clear that the predictions of the blob model presented in Fig. 2 contain some internal contradictions. On the one hand, the picture of the two branches of the free energy meeting at some angle suggests a first order transition. The jumps in the lateral and compression forces are a simple consequence of that. On the other hand, nothing dramatic happens to the chain conformation in the blob picture: the change from a completely confined state to a state with a small escaped tail is continuous, as evidenced in Figs 2e and 2f. The presence of discontinuity in the slope of the fraction of imprisoned monomers suggests that the transition should be classified as second order.

A crucial question to ask is whether one can identify two distinct separate states with a bimodal distribution of some appropriate order parameter. This we address by employing a Monte-Carlo simulation of 2d self-avoiding chains undergoing the escape transition.

V. MONTE CARLO SIMULATION

Single polymer chains grafted in the middle of a strip of length $2L$ and width H are described by SAWs of N steps

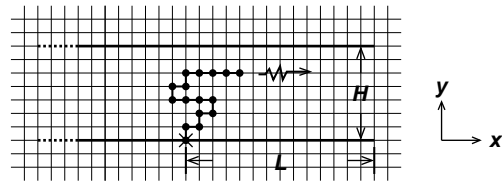


FIG. 3: Schematic drawing of a polymer chain growing as a self-avoiding walk inside a finite strip and grafted at $(x = 0, y = 0)$. Monomers are allowed to sit on the lattice sites except for the lattice sites representing the walls $\{-L \leq x \leq L, y = 0\}$ and $\{-L \leq x \leq L, y = H\}$. The first monomer is attached with a bond to the grafting site marked by a cross. Lengths are measured in units of the lattice spacing.

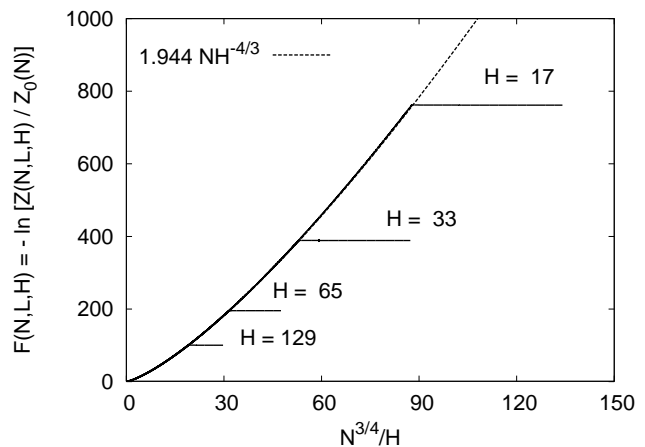


FIG. 4: (a) Free energy relative to a free chain, $F(N, L, H) = -\ln[Z(N, L, H)/Z_0(N)]$, plotted against $N^{3/4}/H$ for $L = 6400$ and $H = 17, 33, 65$, and 129 . The dashed curve is $F_{\text{imp}}(N, L, H) = 1.944NH^{-4/3}$ and gives the best fit of the data.

on a square lattice between two hard walls with distance H as shown in Fig. 3. Monomers are supposed to sit on lattice sites but they are forbidden to sit on the two walls, i.e. $\{-L \leq x \leq L, y = 0\}$ and $\{-L \leq x \leq L, y = H\}$. For our simulations we employ PERM and PERM with k -step Markovian anticipation as described in Ref. [21, 22]. PERM is a biased chain growth algorithm with population control. Polymer chains are built like random walks by adding one monomer at each step. Thus it has the advantage of estimating the partition sum and counting the imprisoned monomers directly.

We simulate 2d SAWs starting at the grafting point of the strip of length $L = 800, 1600, 3200$, and 6400 . The width of the strip is varied from $H = 5$ to $H = 129$. Depending on the chosen sizes of L and H , the total chain length is varied from 2500 to 50000 in order to cover the transition region.

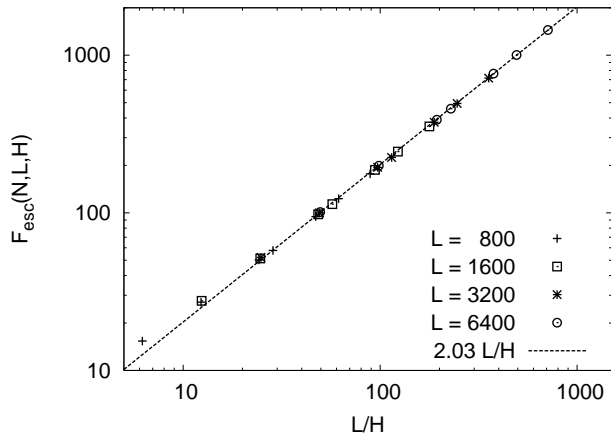


FIG. 5: The log-log plot of the excess free energy of the escaped chain, $F_{\text{esc}}(N, L, H)$, plotted against L/H for various values of L and H . The dashed line is $F_{\text{esc}}(N, L, H) = 2.03L/H$ and gives the best fit of the data.

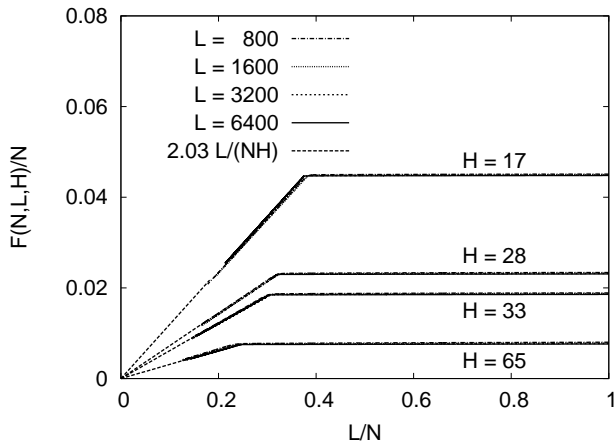


FIG. 6: Free energy relative to a free chain divided by N , $F(N, L, H)/N$, plotted against L/N for various values of L and H . The dashed line extrapolated to zero is $2.03L/(NH)$.

A. Free energy

Let us first discuss the scaling behavior of the free energy. The partition sum of a free SAW in infinite volume for $N \rightarrow \infty$ scales as

$$Z_0(N) = \mu_\infty^{-N} N^{\gamma-1} \quad (18)$$

with μ_∞ being the critical fugacity per monomer, and with $\gamma = 43/32$ being a universal exponent [18]. As chains are still confined in a strip of width H , one should expect the scaling laws of the excess free energy including the crossover from the region of wide strips, $R_F \ll H$, ($R_F \sim N^\nu$ is the Flory radius with $\nu = 3/4$ in $d = 2$), to the region of narrow strips, $R_F \gg H$, where chains are stretched. Since the length of the strip

is finite, here we are more interested in another expected crossover behavior of the excess free energy from an imprisoned and stretched chain state to an escaped state. Therefore, we plot the excess free energy $F(N, L, H) = -\ln(Z(N, L, H)/Z_0(N))$ against $N^{3/4}H^{-1}$ with the precise estimate of $\mu_\infty = 0.37905228$ [23] in Fig. 4. The partition sum $Z(N, L, H)$ is the total number of possible configurations of SAW of N steps partially confined in a strip of length $2L$ and of width H , which is estimated directly in the simulation. In Fig. 4, the sharp crossover behavior from the imprisoned states to the escaped states is indeed seen as N increases for a fixed value of H . The excess free energy of the escaped chain is independent of N , as predicted in a blob picture by Eqs. (13) and (15). The best fit of the free energy for imprisoned state is given by

$$F_{\text{imp}}(N, L, H) \sim 1.944(2)NH^{-4/3}. \quad (19)$$

It is in perfect agreement with the previous estimation in Ref. [22], where the fugacity per monomer scales as $\mu_H - \mu_\infty \sim 0.737H^{-4/3}$ and hence the free energy of the chains of size N in the imprisoned state scales as $F_{\text{imp}} \sim \frac{0.737}{\mu_\infty}NH^{-4/3} \approx 1.944NH^{-4/3}$. Values of the excess free energy of the escaped chain, $F_{\text{esc}}(N, L, H)$ are determined by the horizontal curves shown in Fig. 4. Results for $L = 800, 1600, 3200$ and 6400 are shown in Fig. 5, where we obtain

$$F_{\text{esc}}(N, L, H) = 2.03(3)L/H. \quad (20)$$

As H becomes comparable to L , i.e. $L/H \sim O(10)$, the data points deviate slightly from the straight line, indicating that there are further finite size corrections for small L/H . In order to compare with the theoretical prediction shown in Fig. 2a, we plot $F(N, L, H)/N$ against L/N for various values of L and H in Fig. 6. In the escaped regime, these straight lines extrapolated to $L/N = 0$ are indeed described by Eq. (20) very well. With conventional Monte Carlo simulations it is difficult to estimate the partition sum precisely. With PERM we do have very precise estimates of $Z(N, L, H)$, and therefore we can obtain the lateral and the compression forces by differentiating the estimated free energy, Eqs. (19) and (20), with respect to L and H respectively.

B. Average characteristics of polymer chains

The most straightforward way to understand how the conformations of the polymer chains change as they undergo the escape transition is to estimate the end-to-end distance, $\langle x \rangle$. In Fig. 7, we plot the end-to-end distance per monomer $\langle x \rangle/N$ versus L/N . As long as the polymer chains are imprisoned the curves are horizontal, i.e. the degree of chain stretching is constant, and $\langle x \rangle$ increases linearly with N as shown in Ref. [22]. As the width of the strip, H , decreases, the chains are stretched more. As L/N decreases, we see that there is a jump

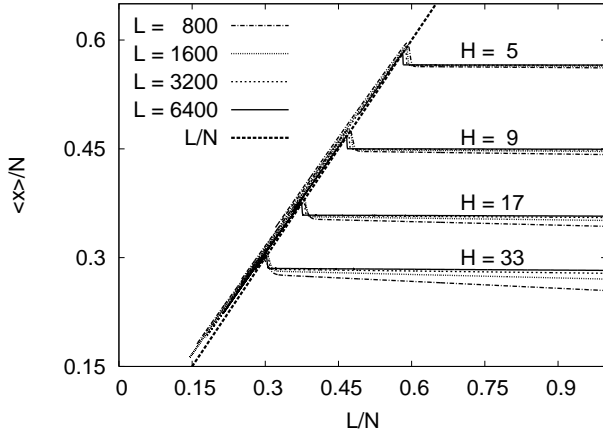


FIG. 7: Average end-to-end distance divided by N , $\langle x \rangle / N$, plotted against L/N for various values of L and H . The dashed line is $\langle x \rangle / N = L/N$.

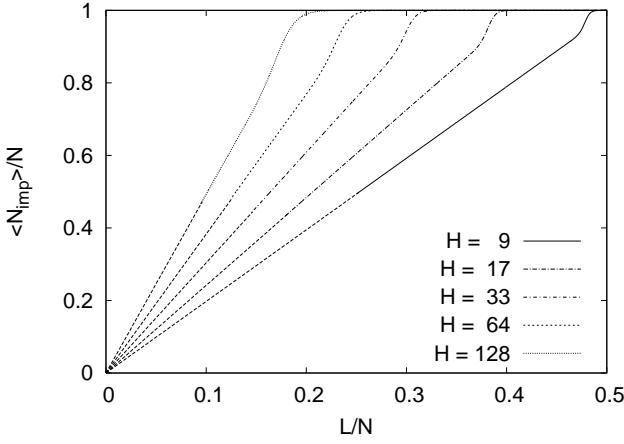


FIG. 8: Average fraction of the imprisoned monomers, $\langle N_{\text{imp}} \rangle / N$, plotted against L/N for $L = 800$ and various values of H . The jump becomes more prominent as H decreases. The ends of the extrapolated straight dashed lines to $L/N = 0$ all approach zero.

in each curve to another branch where $\langle x \rangle = L$. This means that the chain stretching is abruptly increased so that the chain reaches the edge of the strip, indicating that the transition to a partially escaped conformation is first-order like. This is in contrast to the smooth behavior predicted by the blob picture and shown in Fig. 2f.

A jump-wise change in the chain stretching suggests a similar change in the average number of imprisoned monomers, $\langle N_{\text{imp}} \rangle$. In Fig. 8, we plot the fraction of imprisoned monomers $\langle N_{\text{imp}} \rangle / N$ versus L/N for $L = 800$. As long as the chain is imprisoned, $\langle N_{\text{imp}} \rangle / N = 1$. With the increase in the number of monomers, N , each curve indeed develops a jump and the jump becomes more pronounced for smaller H . For a fixed L and $N \rightarrow \infty$, $\langle N_{\text{imp}} \rangle / N \rightarrow 0$ in accord with both theoretical

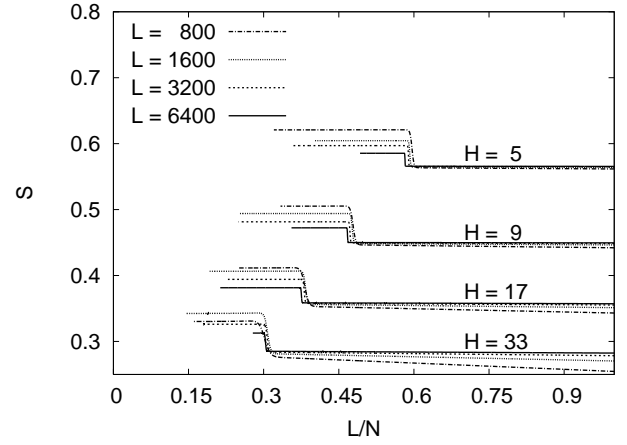


FIG. 9: Average order parameter S plotted against L/N for various values of L and H .

models.

In Fig. 9, we plot the average of the order parameter S , versus L/N . We see clear jumps between the two states. For a given value of H , the order parameter behaves as a step function. The data seem to suggest that the magnitude of the jump decreases with the size of the system, L . A detailed analysis of the distributions of s will be presented in the next section. We will see that the apparent decrease in the jump is due to poor sampling of the escaped state.

C. Transition points

For our simulations the transition points can be determined by analyzing three quantities: (1) free energy, (2) variance of the number of imprisoned monomers N_{imp} , and (3) variance of the end-to-end distance x . Since at the transition point the free energy of the imprisoned state is equal to the free energy of the escaped state, Eqs. (19) and (20) give the following relation between L , N and H at the transition point:

$$\left(\frac{N}{L}\right)_{\text{tr}} = 1.04(2)H^{1/3}. \quad (21)$$

This shows that a polymer chain of size N can be confined in a strip by tuning the length L or the width H of the strip.

The abrupt change scenarios of $\langle x \rangle / N$ and $\langle N_{\text{imp}} \rangle / N$ shown in Fig. 7 and 8 indicate a phase transition but it is difficult to locate precisely the transition point.

It is clear that all the chain configurations can be divided into two subsets: imprisoned and escaped. Far from the transition point, only one subset is important in defining the average characteristics, but in the vicinity of the transition point both subsets contribute, as shown

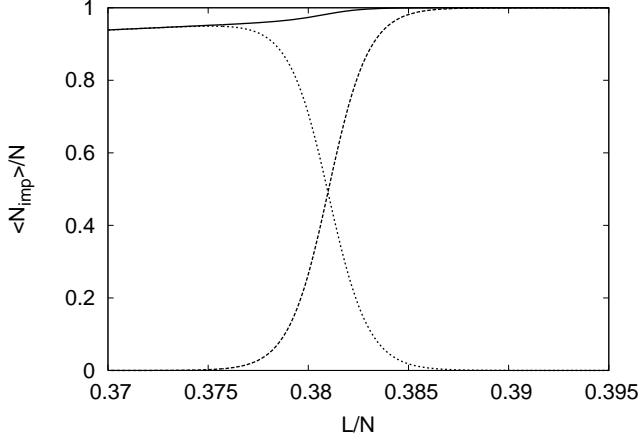


FIG. 10: Average fraction of the imprisoned monomers $\langle N_{\text{imp}} \rangle / N$ (solid line) and two partial contributions, $\langle N_{\text{imp}} \rangle_1 / N$ due to confined configurations, and $\langle N_{\text{imp}} \rangle_2 / N$ due to escaped configurations (dotted lines) as functions of L/N near the transition point $(L/N)_{\text{tr}} = 0.381$ for $L = 3200$ and $H = 17$.

in Fig. 10. The average $\langle N_{\text{imp}} \rangle$ can be rewritten as

$$\begin{aligned} \langle N_{\text{imp}} \rangle &= \frac{\sum_{\{C_1\}} N_{\text{imp}} W_N(C_1) + \sum_{\{C_2\}} N_{\text{imp}} W_N(C_2)}{\sum_{\{C_1\}} W_N(C_1) + \sum_{\{C_2\}} W_N(C_2)} \\ &= \langle N_{\text{imp}} \rangle_1 + \langle N_{\text{imp}} \rangle_2 \end{aligned} \quad (22)$$

where C_1 (C_2) denotes the imprisoned (escaped) configurations, $W_N(C_1)$ ($W_N(C_2)$) are the total weights of the chain for obtaining the configuration C_1 (C_2), and $\langle \dots \rangle_\alpha$ denotes the partial contributions due to the imprisoned configurations ($\alpha = 1$) or the escaped configuration ($\alpha = 2$). Similarly,

$$\langle N_{\text{imp}}^2 \rangle = \langle N_{\text{imp}}^2 \rangle_1 + \langle N_{\text{imp}}^2 \rangle_2. \quad (23)$$

Finally, the variance of N_{imp} , $\sigma^2(N_{\text{imp}}) = \langle N_{\text{imp}}^2 \rangle - \langle N_{\text{imp}} \rangle^2$ can be expressed as follows,

$$\sigma^2(N_{\text{imp}}) = \sigma_1^2(N_{\text{imp}}) + \sigma_2^2(N_{\text{imp}}) - 2 \langle N_{\text{imp}} \rangle_1 \langle N_{\text{imp}} \rangle_2 \quad (24)$$

where $\sigma_{1,2}^2(N_{\text{imp}}) = \langle N_{\text{imp}}^2 \rangle_{1,2} - \langle N_{\text{imp}} \rangle_{1,2}^2$. It is shown in the Appendix that the variances of partial contributions to the total number of imprisoned monomers, $\sigma_1^2(N_{\text{imp}})$ and $\sigma_2^2(N_{\text{imp}})$ are much better suited for locating the transition point than the full variance $\sigma^2(N_{\text{imp}})$ because of the very asymmetric behavior of the latter. We present $\sigma_1^2(N_{\text{imp}})/N$ and $\sigma_2^2(N_{\text{imp}})/N$ as functions of L/N in Fig. 11 for various values of H and L . It is clear that for a fixed width H , the peaks become sharper as the length L of the strip increases. The escape transition points are identified with the positions of the peaks of $\sigma_1^2(N_{\text{imp}})$ and $\sigma_2^2(N_{\text{imp}})$ as determined by a curve fitting. Values of the transition points, $(L/N)_{\text{tr},1}$ and $(L/N)_{\text{tr},2}$ are the same to the third digit for fixed values of L and H , so the transition point is taken as an average of them,

i.e. $(L/N)_{\text{tr}} = ((L/N)_{\text{tr},1} + (L/N)_{\text{tr},2})/2$. Results of $(L/N)_{\text{tr}}$ obtained by this method are listed in Table II and presented in Fig. 12. A more detailed discussion are given in the Appendix. A similar method was also used for determining the transition point from the variance of the end-to-end distance x . Results are also listed in Table II and presented in Fig. 12. All the values of $(N/L)_{\text{tr}}$ are plotted in Fig. 12 against $H^{1/3}$. The best fit gives

$$\left(\frac{N}{L}\right)_{\text{tr}} = 1.025(35)H^{1/3} \quad (25)$$

which is consistent with the estimation of Eq. (21) within the error bar.

VI. LANDAU THEORY: DISTRIBUTION OF THE ORDER PARAMETER

A. Analytical theory

The approach based on the Landau free energy is perfectly suited for analyzing the relevant states in the escape problem, including the metastable states. In the Landau theory, all the configurations are first subdivided into subsets associated with a given value of the order parameter, s , and summation is performed separately within each subset. The full partition function can be obtained then by integrating over the order parameter:

$$Z = \exp(-F) = \int ds \exp(-\Phi(s)) \quad (26)$$

where $\Phi(s)$ is the Landau free energy function, i.e. the non-equilibrium free energy taken as a function of the order parameter. In the vicinity of the first order transition point, the Landau free energy is expected to have two minima (one stable and the other metastable). Our analysis will be based on finding the metastable minima and the associated thermodynamic characteristics. The proper choice of the order parameter is not always obvious, nor are there any standard recipes for making it. One criterion is quite clear: the average value of the order parameter should allow one to distinguish between two phases. For a first-order transition, the average order parameter changes jump-wise. We require that the properly chosen order parameter changes continuously as the system evolves from a metastable state, through the transition state at the top of the barrier, and eventually falls into the equilibrium minimum. We have shown earlier [13] that these criteria are satisfied if the order parameter is defined as the chain stretching in the confined coil state, $s = r/(Na)$ where r is the instantaneous end-to-end distance of the chain of N monomers, or as the stretching of the stem only in the flower conformation: $s = L/(na)$, where n is the number of monomers in the stem. In analogy to the Gaussian case, the Landau function consists of two branches that have to be introduced separately. As the chain is in an imprisoned state,

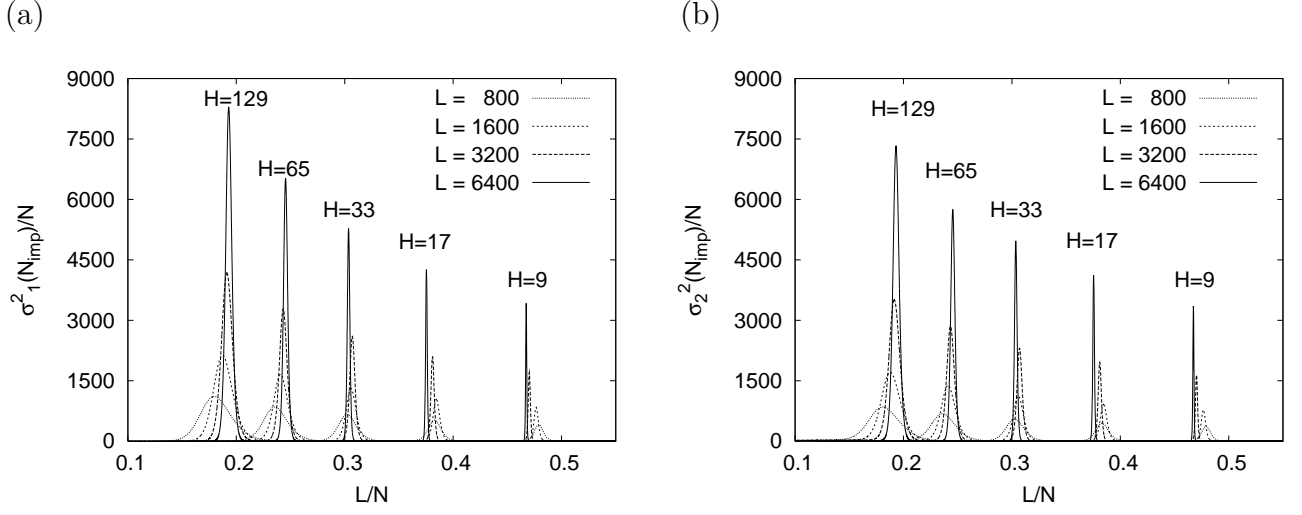


FIG. 11: Variances of the number of imprisoned monomers divided by N , (a) $\sigma_1^2(N_{\text{imp}})/N$, for the imprisoned state, and (b) $\sigma_2^2(N_{\text{imp}})/N$, for the escaped state, plotted against L/N . The height of peaks increases with L for a fixed value of H .

TABLE II: Values of the transition points, $(L/N)_{\text{tr}}$, determined from the analysis of the variances $\sigma_1^2(N_{\text{imp}})$ and $\sigma_1^2(x)$ for the imprisoned states, and from the variances $\sigma_2^2(N_{\text{imp}})$ and $\sigma_2^2(x)$ for the escaped states.

H	$(L/N)_{\text{tr}, N_{\text{imp}}}$				$(L/N)_{\text{tr}, x}$			
	$L = 800$	1600	3200	6400	$L = 800$	1600	3200	6400
9	0.4790	0.4766	0.4703	0.4649	0.4790	0.4766	0.4723	0.4674
17	0.3831	0.3846	0.3810	0.3754	0.3829	0.3836	0.3810	0.3754
33	0.3027	0.3060	0.3071	0.3036	0.3024	0.3078	0.3070	0.3036
65	0.2363	0.2412	0.2434	0.2455	0.2357	0.2409	0.2433	0.2455
129	0.1816	0.1880	0.1916	0.1932	0.1803	0.1877	0.1914	0.1930

the Landau free energy is directly expressed in terms of the distribution of the end-to-end distance. There exists no closed-form formula for such a distribution of confined chains with excluded volume interactions. However, the distribution of the gyration radius for 3d chains confined in a tube was studied analytically and numerically in [24]. It was proposed that the free energy of a confined chain with a given gyration radius r_g can be presented as a sum of two terms:

$$F(r_g) = N \left[A c^\alpha + B \left(\frac{r_g}{Na} \right)^\delta \right], \quad (27)$$

where c is the segment volume concentration expressed as a function of the gyration radius and the confinement geometry, α and δ are linked to the space dimension d and the Flory exponent ν by $\alpha = (\nu d - 1)^{-1}$ and $\delta = (1 - \nu)^{-1}$. The first term describes the concentration effects in the des Cloizeaux [25] form, the second term is the Pincus [26] scaling form of the stretching free energy, and A and B are model-dependent numerical coefficients of order unity. Instead of r_g , we use the same ansatz, Eq. (27), to describe the end-to-end distance distribution

by taking $c = Na^2/rH$, $\alpha = 2$, and $\delta = 4$. The free energy of the chain in an imprisoned state as a function of s is hence given by

$$\Phi_{\text{imp}}(s) = N \left[A \left(\frac{a}{sH} \right)^2 + B s^4 \right], \quad s \leq \frac{L}{Na}. \quad (28)$$

Since we prefer to keep the basic scaling formula of the Landau free energy in order to provide predictions in a simple analytical form, here we are not going to consider the further logarithmic correction terms as shown in [24].

In the thermodynamic limit, the average value of the order parameter for the imprisoned state, S_{imp} , is found by locating the minimum of $\Phi_{\text{imp}}(s)$, i.e. $d\Phi_{\text{imp}}(s)/ds = 0$ at $s = s_{\text{eq}}^{\text{imp}}$, and hence

$$S_{\text{imp}} = s_{\text{eq}}^{\text{imp}} = (A/2B)^{1/6} (a/H)^{1/3}. \quad (29)$$

The minimum of the Landau free energy gives the free energy for the imprisoned state at equilibrium

$$F_{\text{imp}} = \Phi_{\text{imp}}(S_{\text{imp}}) = 3B \left(\frac{A}{2B} \right)^{2/3} \left(\frac{a}{H} \right)^{4/3} N. \quad (30)$$

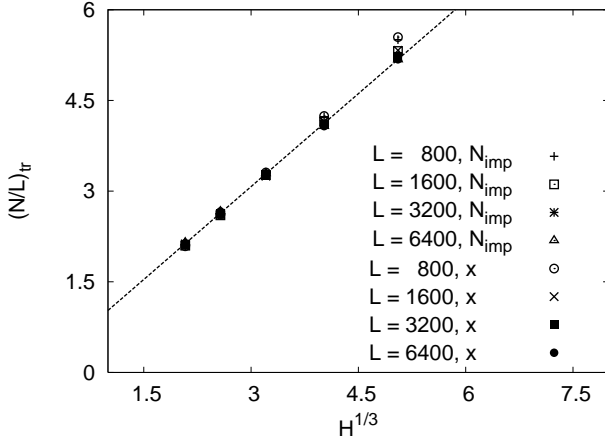


FIG. 12: Transition points $(N/L)_{tr}$ versus H . The dashed line is $(N/L)_{tr} = 1.025(35)H^{1/3}$ and gives the best fit of the data.

Compared with Eq. (13), this is indeed the correct scaling of the free energy. The end-to-end distance at equilibrium is found as

$$R_N = NaS_{imp} = (A/2B)^{1/6}(H/a)^{-1/3}Na, \quad (31)$$

which is consistent with the result of the blob model, Eq. (12).

As the chain is in an escaped state, the formula of the free energy function is identical to Eq. (28), but corrected for the fact that only the n monomers that are part of the stem contribute:

$$\begin{aligned} \Phi_{esc}(s) &= n \left[A \left(\frac{a}{sH} \right)^2 + Bs^4 \right] \\ &= \frac{L}{a} \left[A \left(\frac{a}{H} \right)^2 s^{-3} + Bs^3 \right], \quad s \geq \frac{L}{Na}. \end{aligned} \quad (32)$$

The average value of the order parameter in the escaped state, S_{esc} , is found by locating the minimum of $\Phi_{esc}(s)$ and is given by

$$S_{esc} = s_{eq}^{imp} = (A/B)^{1/6}(a/H)^{1/3} \quad (33)$$

Thus, the free energy of the escaped chain at equilibrium is

$$F_{esc} = \Phi_{esc}(S_{esc}) = 2(AB)^{1/2} \left(\frac{L}{H} \right) \quad (34)$$

The transition point is found from the condition that the two minima of the Landau free energy function are of equal depth. Using Eqs. (30) and (34) we get

$$\left(\frac{L}{Na} \right)^* = \frac{3}{2^{5/3}} \left(\frac{A}{B} \right)^{1/6} \left(\frac{a}{H} \right)^{1/3} \quad (35)$$

It is interesting to calculate the size of jumps implied by the Landau theory in the order parameter, the imprisoned monomers and the end-to-end distance at the

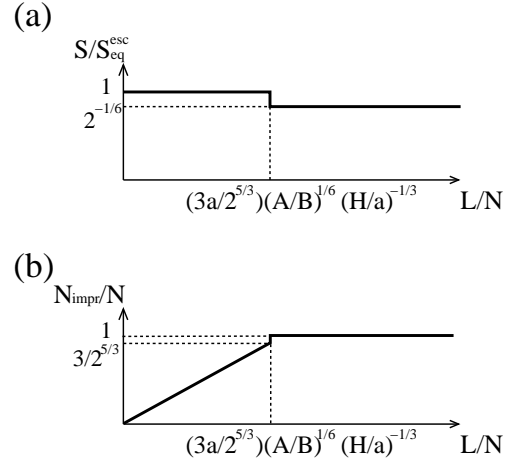


FIG. 13: Based on the Landau theory, the theoretical predictions of the average values of (a) the fraction of imprisoned monomers N_{imp}/N , and (b) the order parameter S , are plotted against L/N . The chain is in an imprisoned state for $L/N > (3a/2^{5/3})(A/B)^{1/6}(a/H)^{1/3}$, and in an escaped state for $L/N < (3a/2^{5/3})(A/B)^{1/6}(a/H)^{1/3}$.

transition. Using Eqs. (29) and (33) we immediately get the reduced jump of the order parameter

$$\frac{\Delta S}{S_{esc}} = \frac{S_{esc} - S_{imp}}{S_{esc}} = 1 - 2^{-1/6} \approx 0.1091, \quad (36)$$

which is independent of H and the coefficients A and B . For an imprisoned state, $\langle N_{imp} \rangle = N$ by definition, while for the coexisting escaped state with the same choice of H , L , and N we have only $\langle N_{imp} \rangle = L/S_{esc}$ monomers. From Eqs. (33) and (35), we obtain the relative reduction in the number of imprisoned monomers

$$\frac{\Delta N_{imp}}{N} = \frac{N - L/S_{esc}}{N} = 1 - \frac{3}{2^{5/3}} \approx 0.055. \quad (37)$$

This number has a simple meaning of the fraction of the chain escaping out of the confinement at the transition point. It is much smaller than 1/2 in the Gaussian chain model, but non-zero in contrast to the blob model. Finally, the reduced jump of the end-to-end distance is obtained by combining Eqs. (31) and (35)

$$\frac{\Delta R}{L} = \frac{L - R_N}{L} = 1 - \frac{2^{3/2}}{3} \approx 0.0572. \quad (38)$$

Eqs. (36)-(38) show that the sizes of jumps in S , $\langle N_{imp} \rangle / N$ and R_N/L are universal quantities. Results for the average order parameter S and the average fraction of imprisoned monomers $\langle N_{imp} \rangle / N$ predicted by the Landau theory are shown in Fig.13. Comparing with the numerical results shown in Fig. 8 and Fig.9, we see that the Landau theory a good qualitative agreement.

The predicted free energy of the chain at equilibrium, Eqs. (30) and (34) follow the same scaling behavior as

obtained by the MC simulations shown in Eqs. (19) and (20). This allows us to identify the numerical values of the constants A and B for our model: $A \approx 1.057$ and $B \approx 0.975$.

B. Numerical comparisons

Here we focus on the results of the Landau free energy of polymer chains partially confined in a strip of width $H = 28$ and of length $L = 800, 1600, 3200$, and 6400 . Since PERM gives the possibility to estimate directly the partition sum and the properly normalized histograms, the Landau free energy as a function of s , $\Phi(N, L, H, s)$, is given by

$$\Phi(N, L, H, s) = -\ln \left(\frac{P(N, L, H, s)}{Z_0(N)} \right) \quad (39)$$

where $P(N, L, H, s) = \sum_{walks} \delta_{s,s'}$ is the histogram of s , and the partition sum of the partially confined chains can be written as

$$Z(N, L, H) = \sum_s P(N, L, H, s) \quad (40)$$

in accordance with Eq. (26). In Fig. 14, we plot four sets of results of the Landau free energy per monomer $\Phi(N, L, H, s)/N$ versus the order parameter s for $L = 800, 1600, 3200$ and 6400 . Since the transition point is near $H^{1/3}$, the histograms are obtained for $N/L = 3.05, 3.10$ and 3.15 for each set. The predicted analytical results of $\Phi^P(s) = \Phi_{\text{imp}}(s)$ for the imprisoned state and $\Phi^P(s) = \Phi_{\text{esc}}(s)$ for the escaped state, given by Eqs. (28) and (32) are also shown for comparison. On the left-hand side of the branch points, due to the finite-size effect, we see that the excess free energy for the imprisoned state (the minimum of the curve) at $s = s_{\text{eq},L}^{\text{imp}}$ converges to the predicted value (the minimum of the curve $\Phi^P(s)$) of polymer chains confined in an infinite strip at $s = s_{\text{eq}}^{\text{imp}}$ slowly as L increases but $s_{\text{eq},L}^{\text{imp}}$ is slightly larger than $s_{\text{eq}}^{\text{imp}}$ as $L \rightarrow \infty$. The difference between those curves corresponding to the different ratio N/L is almost invisible for a fixed value of L as predicted by Eq. (28). On the right-hand side of the branch points, we see that only those curves for $L = 800$ finally develop a parabola-like behavior with fluctuations and they are more concave than those curves predicted by Eq. (32). It shows that PERM has difficulties to sample configurations in the escaped regime as L increases and gives an explanation why we should not trust the size of those jumps that appear in Fig. 9 too much. However, one can easily overlook the existence of two minima in such a delicate situation. With PERM, at least we are able to give evidence for this two minimum picture of the first-order like transition. We also see that additional finite-size correction terms should be taken into account for the theoretical predictions in Eqs. (28) and (32).

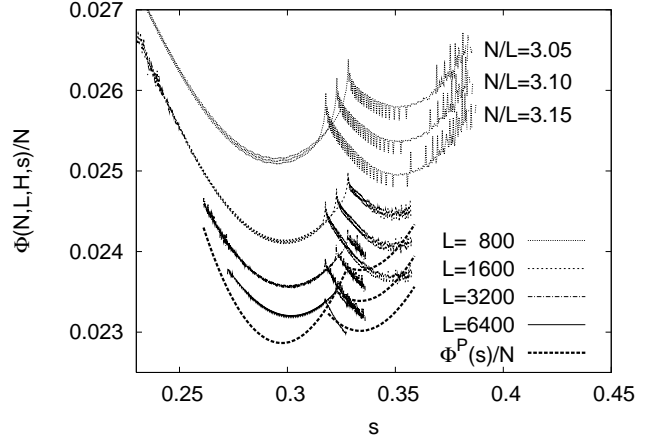


FIG. 14: The Landau free energy divided by N , $\Phi(N, L, H, s)/N$, plotted against s for various values of L and $H = 28$. The predicted Landau free energy functions, $\Phi^P(s) = \Phi_{\text{imp}}$, Eq. (28), in the imprisoned regime and $\Phi^P(s) = \Phi_{\text{esc}}$, Eq. (32), in the escaped regime are also plotted (dashed lines).

Taking the results for $L = 6400$ as a reference, we plot the same data but shift all other curves by some constants, $c_{0,L} = -0.00235, -0.00109, -0.00044$ for $L = 800, 1600$, and 3200 to make the three branch points for $N/L = 3.05, 3.10$, and 3.15 coincide with each other in Fig. 15. According to the prediction by Eq. (28), we should expect that the four curves for different values of L overlap with each other in the imprisoned regime. In fact, it is not the case but the difference between these curves decreases as L increases, and finally they will converge to one curve as L becomes very large. In the escaped regime, surprisingly, we see that those curves corresponding to different L all overlap with each other for a fixed ratio of N/L as predicted by Eq. (32). Although the lack of data for larger L , precludes very strong conclusions, we may assume that these curves all show the same behavior as the curve for $L = 800$, and do further analysis.

In order to determine the transition point and extract an accurate value for the jump in the order parameter from simulations, we use two parabolic functions $g_{\text{imp}}(s)$ and $g_{\text{esc}}(s)$ to fit the numerical data in the imprisoned and escaped regimes, respectively:

$$g_{\text{imp}}(s) = a_{1,L}(s - s_{\text{eq},L}^{\text{imp}})^2 + c_{1,L} \quad (41)$$

and

$$g_{\text{esc}}(s) = a_2(s - s_{\text{eq},L}^{\text{esc}})^2 + c_2 + b_2 \frac{N}{L} \quad (42)$$

where $a_{1,L}, c_{1,L}, a_2, c_2, b_2, s_{\text{eq},L}^{\text{imp}}$, and $s_{\text{eq},L}^{\text{esc}}$ are determined by curve fitting, and results are shown in Table III and Fig. 15. From the condition of equal depth of minima

$$g_{\text{imp}}(s = s_{\text{eq},L}^{\text{imp}}) = g_{\text{esc}}(s = s_{\text{eq},L}^{\text{esc}}), \quad (43)$$

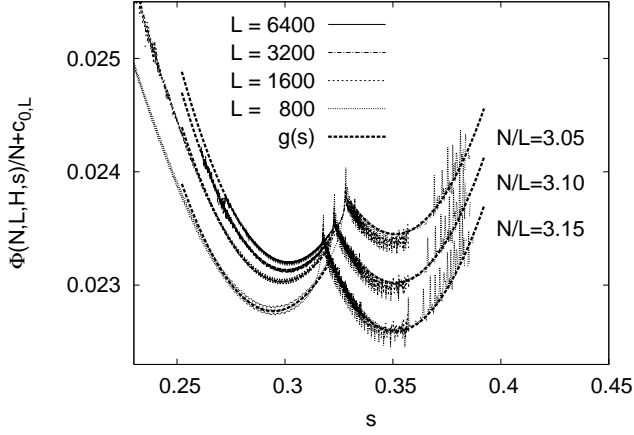


FIG. 15: The Landau free energy divided by N , $\Phi(N, L, H, s)/N$, plotted against s for various values of L and $H = 28$. The two minima of $\Phi(N, L, H, s)/N$ are determined by fitting $g(s) = g_{\text{imp}}(s)$, Eq. (41), in the imprisoned regime, and $g(s) = g_{\text{esc}}(s)$, Eq. (42), in the escaped regime, going through those lower points around the two minima, respectively.

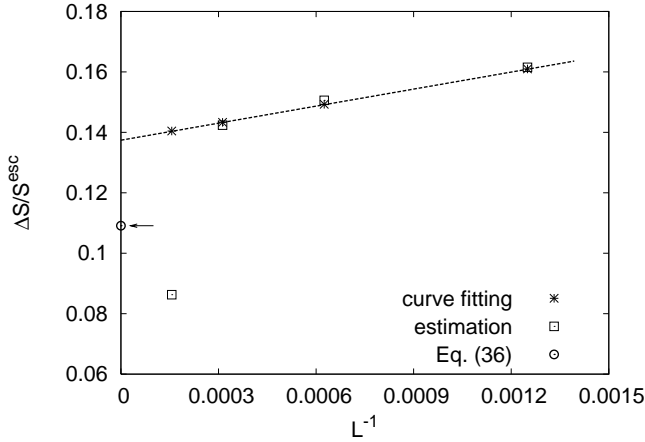


FIG. 16: The reduced jump of the order parameter $\Delta S/S_{\text{esc}}$ plotted against L^{-1} .

we obtain the transition points $(N/L)_{\text{tr}} = 3.13(2)$, $3.10(2)$, $3.09(1)$, and $3.08(1)$ for $L = 800$, 1600 , 3200 , and 6400 , respectively, which are in perfect agreement with the results given by free energy, Eq. (21), and the results given by the variance of the end-to-end distance and the imprisoned monomers, Eq. (25).

The values for the reduced jump of the order parameter,

$$\frac{\Delta S}{S_{\text{esc}}} = \frac{s_{\text{eq},L}^{\text{esc}} - s_{\text{eq},L}^{\text{imp}}}{s_{\text{eq},L}^{\text{esc}}} \quad (44)$$

obtained by the curve fitting are plotted in Fig 16 against L^{-1} together with the direct estimates in the simulations

TABLE III: Results of the coefficients $a_{1,L}$, $c_{1,L}$, a_2 , c_2 , b_2 , $s_{\text{eq},L}^{\text{imp}}$, and $s_{\text{eq},L}^{\text{esc}}$ for the curve fitting in Fig. 15.

L	$a_{1,L}$	$c_{1,L}$	$s_{\text{eq},L}^{\text{imp}}$	a_2	c_2	b_2	$s_{\text{eq},L}^{\text{esc}}$
800	0.6281	0.02277	0.2945	0.6518	0.0497	-0.0086	0.3510
1600	0.6336	0.02303	0.2986				
3200	0.6675	0.02313	0.3007				
6400	0.6872	0.02320	0.3017				

and the prediction by the analytical theory, Eq. (36). We see that $\Delta S/S_{\text{esc}}$ decreases as L increase. As $L \rightarrow \infty$, it remains finite and the value is slightly larger than the predicted value by the analytical theory. However, in view of the numerical uncertainties of our curve fitting we consider that the predictions of the analytical theory and the results by the MC simulations agree with each other quite well.

VII. SUMMARY AND DISCUSSION

In this paper we attack the problem of the 2d-escape transition by combining several approaches. We first compare two simple pictures of the transition predicted for Gaussian chains and by a blob model. This comparison is useful from a general pedagogical point of view since the two models are in a sense complementary: each captures some essential features of the phenomenon while failing in some other aspects. Both models are attractive because of their clarity, and although mathematically simple, lead to non-trivial results including finite-size effects in a phase transition. The third approach that was proposed in this paper attempts at incorporating the excluded volume effects in the framework of the Landau theory. We were not able to present an exact theory since it would require a detailed understanding of the end-to-end distribution of confined self-avoiding chains. To the best of our knowledge this problem is still not well explored. The simulations presented allowed us to evaluate the transition condition Eq. (21) which represents the binodal line in the $(H, L/N)$ plane. It is of interest to extend the simulations in order to locate the spinodal lines where one of the states loses stability, and to construct the full phase diagram. It is also possible to explore the properties of metastable states and their lifetimes controlled by the barrier heights. It is clear from the results on the distribution of the order parameter, Fig. 14, that the PERM algorithm experiences difficulties with sampling the configurations belonging to the escaped state, especially for long chains. The escaped branch of the distribution is cut-off quite sharply, which means that the important set of configurations characterized by larger stretching degree in the stem is vastly underrepresented. This is a generic problem that one encounters when dealing with first-order transitions when

the properties of the phases differ significantly. In our case, the PERM algorithm based on chain growth technique is perfectly tuned to generate homogeneous configurations of imprisoned chains but fails with strongly inhomogeneous escaped configurations. It is worth noting that a naive determination of the jumps in the average order parameter would have lead one to a wrong conclusion that the jump disappears in the thermodynamic limit. Again, we expect this to be a generic problem when simulating weak first-order transitions. The most reliable analysis of the nature of the transition would require a detailed examination of the order parameter distribution.

Acknowledgements

We are grateful to the Deutsche Forschungsgemeinschaft (DFG) for financial support: H.-P.H. was supported under grant NO SFB 625/A3, while L.I.K. and A.M.S. received partial support under grants NO 436 RUS 113/863/0 and RFBR 05-03-32003-a. H.-P.H. thanks P. Grassberger and W. Paul for very helpful discussions.

Appendix

In this appendix, we discuss the finite-size behavior in the fluctuations in the number of imprisoned monomers N_{imp} in more detail. Following the technique of finite-size scaling analysis for first-order transitions as described in [27], we write down the probability distribution of the fraction of imprisoned monomers $m = N_{\text{imp}}/N$ in the two-state model

$$P(m) = \delta(m - m_1) \frac{e^{(t-t_{\text{tr}})a}}{e^{(t-t_{\text{tr}})a} + e^{-(t-t_{\text{tr}})a}} + \frac{1}{\sqrt{2\pi}\sigma_0} e^{-\frac{(m-m_2)^2}{2\sigma_0^2}} \frac{e^{-(t-t_{\text{tr}})a}}{e^{(t-t_{\text{tr}})a} + e^{-(t-t_{\text{tr}})a}}. \quad (45)$$

The first term accounts for the imprisoned state with m strictly equal to $m_1 = 1$, while the second term describes the distribution of m in the escaped state in the Gaussian approximation with the equilibrium average of m equal to m_2 and dispersion σ_0 ; t is the control parameter, t_{tr} is its critical value at the transition point, and $P(m)$ is normalized,

$$\int P(m) dm = 1 \quad (46)$$

At the transition point $t = t_{\text{tr}}$,

$$P(m) = \frac{1}{2} \left[\delta(m - m_1) + \frac{1}{\sqrt{2\pi}\sigma_0} e^{-\frac{(m-m_2)^2}{2\sigma_0^2}} \right] \quad (47)$$

which obeys the “equal-weight rule”, while for $t \neq t_{\text{tr}}$ the relative weight of the two states is $\exp[2(t - t_{\text{tr}})a]$.

The constant a^{-1} describes the range of t over which the transition is smeared out. For the Gaussian approximation to be meaningful the dispersion of m in the escaped state, σ_0 , must be small compared to the difference $\Delta m = m_1 - m_2$. Taking $t = L/N$ and using Eqs. (30), (32), and (34) of the Landau theory, one expects the following scaling: $a^{-1} \sim H^{2/3}/L$ and $\sigma_0^2 \sim H/L$.

Since the probability density is a sum of two contributions, $P(m) = P_1(m) + P_2(m)$, the k -th moment of m is defined by

$$\langle m^k \rangle = \int m^k P(m) dm = \langle m^k \rangle_1 + \langle m^k \rangle_2 \quad (48)$$

where $\langle m^k \rangle_{1,2} = \int m^k P_{1,2}(m) dm$. Therefore, the first and second moment are given by

$$\langle m \rangle = m_1 p_1 + m_2 p_2, \quad (49)$$

and

$$\langle m^2 \rangle = m_1^2 p_1 + (m_2^2 + \sigma_0^2) p_2, \quad (50)$$

here $p_1 = e^{(t-t_{\text{tr}})a}/2 \cosh[(t-t_{\text{tr}})a]$ is the relative weight of the imprisoned state, and $p_2 = 1 - p_1$ is the relative weight of the escaped state.

Instead of a δ -function singularity at $t = t_{\text{tr}}$, the variance of the fraction of imprisoned monomers in a finite system becomes

$$\langle m^2 \rangle - \langle m \rangle^2 = p_1 p_2 (\Delta m)^2 + p_2 \sigma_0^2 \quad (51)$$

which shows a smooth asymmetric peak close to $t = t_{\text{tr}}$ of approximate height $\Delta m^2 + \sigma_0^2$. Here Δm is the relative reduction in the number of imprisoned monomers at the transition point, for which the analytical Landau theory predicts a value of 0.055, see Eq. (37). The first term in Eq. (51) is symmetric with respect to the transition point since $p_1 p_2 = 1/(4 \cosh^2[(t-t_{\text{tr}})a])$. The second term, however, is asymmetric, as it describes the intrinsic fluctuations in the escaped state. The resultant asymmetry is clearly seen in Fig. 17. We conclude that the full variance of m is ill suited for a precise determination of the transition point.

The situation is quite different if we analyze the variances calculated with the partial probability densities $P_1(m)$ and $P_2(m)$ restricted to the imprisoned (escaped) configurations. In the simulations, the product $N\sigma_{1,2}^2$ was calculated. The variance due to the imprisoned configurations only (with $m_1 = 1$) gives a perfectly symmetric curve as a function of the control parameter:

$$N\sigma_1^2(m) = N m_1^2 p_1 p_2 = \frac{N^2}{4 \cosh^2[(t-t_{\text{tr}})a]} \quad (52)$$

with the peak value of $N_{\text{tr}}/4 \approx LH^{1/3}/4$. Numerical data presented in Fig. 18 supports this prediction with very high accuracy. The variance due to escaped configurations is somewhat modified by the intrinsic fluctuations

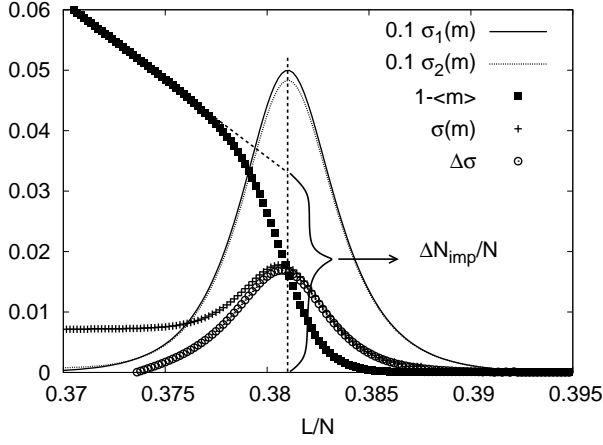


FIG. 17: The square root of the variance $\sigma_1(m)$ for the imprisoned states, $\sigma_2(m)$ for the escaped chains, $1 - \langle m \rangle$, $\sigma(m)$ of the chain either in an imprisoned state or in an escaped state, and the difference $\Delta\sigma = \sigma_1(m) - \sigma_2(m)$ against L/N .

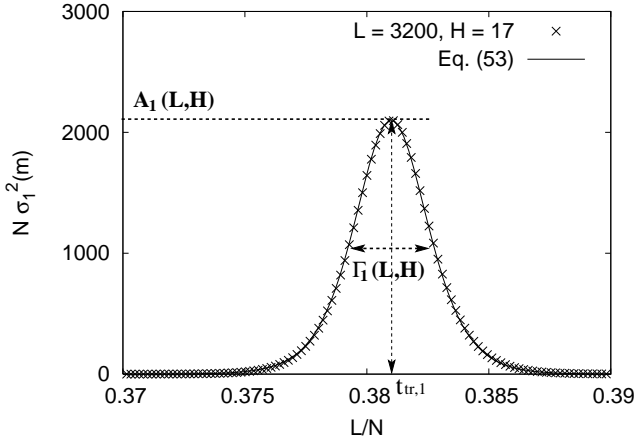


FIG. 18: Variance due to the imprisoned configuration multiplied by N , $N\sigma_1^2(m)$, plotted against L/N for $L = 3200$ and $H = 17$. The solid curve is the best fit of Eq. (52), $Nm_1^2/4\cosh^2[(t - t_{tr})a]$, with the height of the peak $A_1(L, H) = N(m_1)^2/4 \approx 2099.74$, the FWHM $\Gamma_{\text{imp}}(L, H) \approx 1.7627/a = 0.0035$, and the position of the peak $t_{tr,1} = (L/N)_{tr,1} = 0.3810$. The FWHM are given by the distance between points on the curve shown at which the corresponding height reaches half height of the peaks (half maximum).

in the escaped state

$$N\sigma_2^2(m) = N(m_2^2 p_1 p_2 + p_2 \sigma_0^2) \approx Nm_2^2 p_1 p_2 = \frac{N(1 - \Delta m)^2}{4 \cosh^2[(t - t_{tr})a]} \quad (53)$$

but in contrast to Eq. (51), the asymmetric term is always negligible. Indeed, the coefficient with the symmetric term, $m_2^2 = (1 - \Delta m)^2$ is close to 1 while both quantities $(\Delta m)^2$ and σ_0^2 are quite small. In Fig. 17,

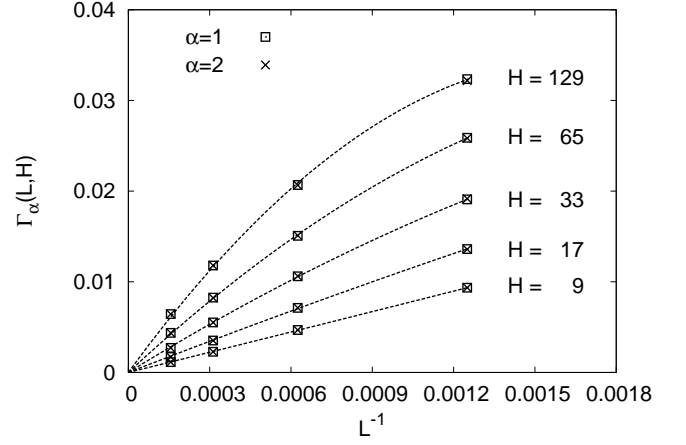


FIG. 19: FWHM $\Gamma_\alpha(L, H)$ for the imprisoned state ($\alpha = 1$) and for the escaped state ($\alpha = 2$) against L^{-1} . The dashed curves are $a_{1,H}(H/L) + b_{1,H}(H/L)^2$ and give the best fit of the data. Values of $a_{1,H}$ and $b_{1,H}$ are listed in Table IV.

TABLE IV: Results of the coefficients $a_{1,H}$, $b_{1,H}$, $a_{2,H}$, $c_{2,H}$ and $d_{2,H}$ for the curve fitting in Fig. 19 and 20.

H	$a_{1,H}$	$b_{1,H}$	$a_{2,H}$	$c_{2,H}$	$d_{2,H}$
9	0.8221	0.7841	0.9940	0.2131	2.2802
17	0.6845	-2.0403	0.9845	0.0961	0.4540
33	0.5600	-2.3531	0.9725	0.0430	0.0570
65	0.4301	-1.3774	0.9545	0.0173	0.0095
129	0.3185	-0.7332	0.9220	0.0070	0.0017

we plot the full dispersion $\sigma(m)$ (the square root of the full variance) that includes contributions from all configurations, and partial dispersions $\sigma_1(m)$ and $\sigma_2(m)$ due to imprisoned and escaped configurations separately, the difference $\Delta\sigma = \sigma_1(m) - \sigma_2(m)$, as well as the average fraction of escaped monomers, $1 - \langle m \rangle$, as functions of L/N . It is clear that the full curve is strongly asymmetric in contrast to partial dispersion curves, in good agreement with the theoretical description above. On the other hand, the curve of $\Delta\sigma$ shows the same behaviour as the curve of $\sigma(m)$ near the transition point, and the heights of these two peaks correspond to the half size of the jump $\Delta m = m_1 - m_2 = \Delta N_{\text{imp}}/N$. By fitting the partial variances $N\sigma_1^2(m)$ and $N\sigma_2^2(m)$ as functions of L/N according to Eqs. (52) and (53), respectively, we obtain the full width at half-maximum (FWHM), $\Gamma(L, H) = 2\text{arccosh}(\sqrt{2})/a$, the height of the peak $A_\alpha(L, H) = Nm_\alpha^2/4$, and the transition point $t_{tr,\alpha} = (L/N)_{tr,\alpha}$ for $\alpha = 1$ (imprisoned configurations) and $\alpha = 2$ (escaped configurations).

One example of the curve fitting for $L = 3200$ and $H = 17$ is shown in Fig. 18. Note that the peak height and the transition point are related to the theoretical prediction $A_1(L, H) \approx LH^{1/3}/4$ with very high accuracy.

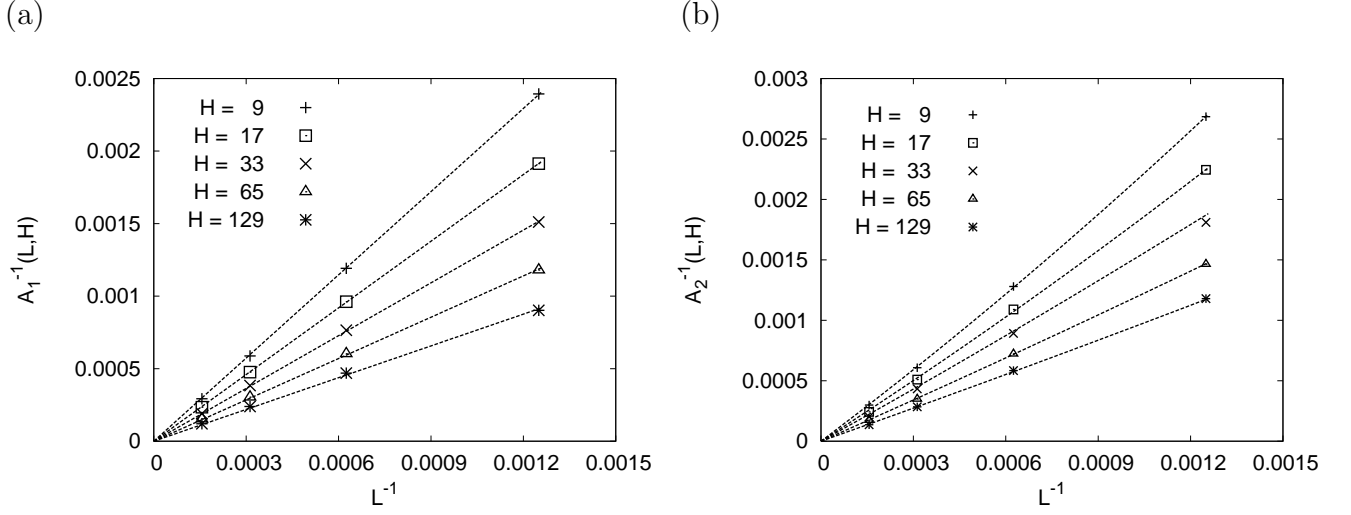


FIG. 20: Inverse of the height of the peaks for the imprisoned state (a) $A_1^{-1}(L, H)$, and for the escaped state (b) $A_2^{-1}(L, H)$, plotted against L^{-1} . The dashed curves are (a) $a_{2,H}(4H^{-1/3}/L)$ and (b) $c_{2,H}(H/L) + d_{2,H}(H/L)^2$, and give the best fit of the data. Values of $a_{2,H}$, $c_{2,H}$, and $d_{2,H}$ are listed in Table IV.

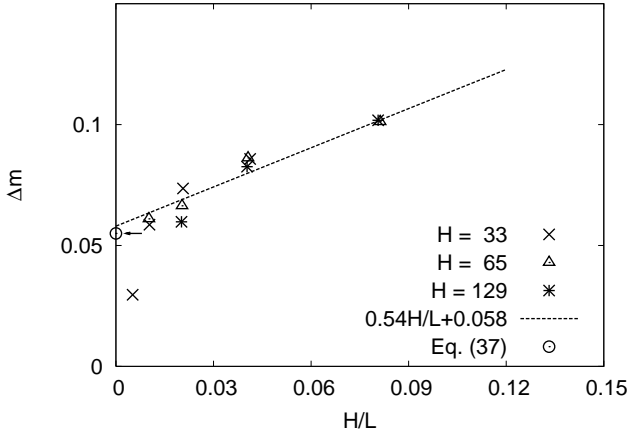


FIG. 21: The relative reduction in the number of imprisoned monomers Δm , plotted against H/L .

Results of $\Gamma_\alpha(L, H)$, $A_\alpha(L, H)$ for $\alpha = 1$ and for $\alpha = 2$, and $t_{tr,\alpha}$ are shown in Fig. 19, 20 and 12. In Fig. 19, we see that the full widths $\Gamma_\alpha(L, H)$ for $\alpha = 1$ and for $\alpha = 2$

are overlapped with each other, and $\Gamma_\alpha \rightarrow 0$ as $1/L \rightarrow 0$ by fitting the data using $a_{1,H}(H/L) + b_{1,H}(H/L)^2$. In Fig. 20, the inverse of the height $A_1^{-1}(L, H) \rightarrow 0$ as $1/L \rightarrow 0$ by fitting the data using $a_{1,H}(4H^{-1/3}/L)$ and $c_{1,H}(H/L) + d_{1,H}(H/L)^2$. Since $\Gamma_\alpha \rightarrow 0$, and $A_\alpha^{-1} \rightarrow 0$ as $1/L \rightarrow 0$, i.e. a delta function, a sharp phase transition occurs in the thermodynamic limit. It is a strong indication [27] that the transition is first-order like. Values of the coefficients $a_{1,H}$, $b_{1,H}$, $a_{2,H}$, $c_{2,H}$ and $d_{2,H}$ are listed in Table IV.

The relative reduction in the number of imprisoned monomers

$$\begin{aligned} \Delta m &= m_1 - m_2 \\ &= 2(A_1^{1/2} - A_2^{1/2})/N^{1/2} \end{aligned} \quad (54)$$

Results of Δm for various values of H and L plotted against H/L are shown in Fig. 21. We see that there exist the systematic errors at small H/L . Finally we obtain $\Delta m \approx 0.058$ at $H/L \rightarrow 0$ by a curve fitting, which is slightly larger than the prediction, Eq. (37).

-
- [1] G. Subramanian, D. R. M. Williams and P. A. Pincus, Europhys. Lett. **29**, 285 (1995); Macromolecules **29**, 4045 (1996).
 - [2] J. Ennis, E. M. Sevick and D. R. M. Williams, Phys. Rev. E **60**, 6906 (1999).
 - [3] E. M. Sevick and D. R. M. Williams, Macromolecules, **32**, 6841 (1999).
 - [4] B. M. Steels, F. A. M. Leermakers, and C. A. Haynes. J. Chrom. B. **743**, 31 (2000).
 - [5] A. Milchev, V. Yamakov and K. Binder, Phys. Chem. Chem. Phys. **1**, 2083 (1999); Europhys. Lett. **47**, 675 (1999).
 - [6] J. Jimenez and R. Rajagopalan, Langmuir. **14**, 2598 (1998).
 - [7] E. M. Sevick, Macromolecules **33**, 5743 (2000).
 - [8] J. Ennis, and E. M. Sevick, Macromolecules **34**, 1908 (2001).
 - [9] D. R. M. Williams and F. C. MacKintosh, J. Phys. II

- France **9**, 1417 (1995).
- [10] M. C. Guffond, D. R. M. Williams, and E. M. Sevick, *Langmuir*. **21**, 5691 (1997).
 - [11] F. A. M. Leermakers, and A. A. Gorbunov, *Macromolecules* **35**, 8640 (2002).
 - [12] J. Abbou, A. Anne, and K. Demaille, *J. Phys. Chem.* **110**, 22664 (2006).
 - [13] A. M. Skvortsov, L. I. Klushin, and F. A. M. Leermakers., *Europhys. Lett.* **58**, 292 (2002).
 - [14] L. I. Klushin, A. M. Skvortsov and F. A. M. Leermakers. *Phys. Rev. E* **69**, 061101 (2004).
 - [15] F. A. M. Leermakers, A. M. Skvortsov, and L. I. Klushin., *J. Stat. Mech.: Theor. Exp.* 10001, 1 (2004).
 - [16] A. M. Skvortsov, L. I. Klushin, and F. A. M. Leermakers, *Macromol. Symp.* **237**, 73 (2006); *J. Chem. Phys.* **126**, 024905 (2007).
 - [17] A. Y. Grosberg and A. R. Khokhlov, "*Statistical Physics of Macromolecules*", Oxford University Press, New York, 1994.
 - [18] E. Eisenriegler, "*Random Walks in Polymer Physics*", *Lecture Notes in Physics*, Vol.508, Springer, New York, 1998.
 - [19] G. J. Fleer, J. M. H. M. Scheutjens, M. A. Cohen Stuart, T. Cosgrove, and B. Vincent, "*Polymers at Interfaces*" (Chapman & Hall, London, 1993).
 - [20] P. G. de Gennes, "*Scaling Concepts in Polymer Physics*" ; (Cornell University Press Ithaca, New York, 1979).
 - [21] P. Grassberger, *Phys. Rev. E* **56**, 3682 (1997).
 - [22] H.-P. Hsu and P. Grassberger, *Eur. Phys. J.* **B36**, 209-214 (2003).
 - [23] A. R. Conway and A. J. Guttmann, *Phys. Rev. Lett.* **77**, 5284 (1996).
 - [24] P. Sotta, A. Lesne, and J. M. Victor, *J. Chem. Phys.* **112**, 1565 (2000).
 - [25] J. des Cloizeaux, *J. Phys. (Paris)* **41**, 223 (1980).
 - [26] P. Pincus, *Macromolecules* **9**, 386 (1976).
 - [27] K. Binder and D. P. Landau, *Phys. Rev. B* **30**, 1477 (1984).